ESC HEART FAILURE
ESC Heart Failure 2022; **9**: 3031–3043
Published online 23 June 2022 in Wiley Online Library (wileyonlinelibrary.com) **DOI:** 10.1002/ehf2.14034

ORIGINAL ARTICLE

Histopathological and epigenetic changes in myocardium associated with cancer therapy-related cardiac dysfunction

Chiyoko-Ikeda Terada[1], Kenji Onoue[2]*, Tomomi Fujii[1], Hiroe Itami[1], Kohei Morita[1], Tomoko Uchiyama[1], Maiko Takeda[1], Hitoshi Nakagawa[2], Tomoya Nakano[2], Youichirou Baba[3], Kisaki Amemiya[4], Yoshihiko Saito[2], Kinta Hatakeyama[1,4]* and Chiho Ohbayashi[1]

[1]*Department of Diagnostic Pathology, Nara Medical University, 840 Shijo, Kashihara, Nara, 643-8522, Japan;* [2]*Department of Cardiovascular Medicine, Nara Medical University, 840 Shijo, Kashihara, Nara 634-8522, Japan;* [3]*Department of Pathology, Suzuka General Hospital, 1275-53 Yasuduka, Suzuka, Mie 513-8630, Japan; and* [4]*Department of Pathology, National Cerebral and Cardiovascular Center, 6-1 Kishibe-Shimmachi, Suita, Osaka 564-8565, Japan*

Abstract

Aims Cancer therapy-related cardiac dysfunction (CTRCD) is commonly reported, but its histopathology, mechanisms, and risk factors are not known. We aimed to clarify the histopathology and mechanisms of CTRCD to identify risk factors.

Methods and results We performed myocardial histopathological studies on 13 endomyocardial biopsies from CTRCD patients, 35 autopsied cancer cases with or without cardiac dysfunction, and controls without cancer (10 biopsies and 9 autopsies). Cardiotoxicity risk scores were calculated based on medication; and patient-related risk factors, fibrosis, and cardiomyocyte changes were scored; and p53 and H3K27ac histone modification were evaluated by histological score (H-score). In the biopsy cases, all histopathological changes and the p53 evaluation were significantly higher in the CTRCD group than in the controls [p53 H-score; 63 (9.109) vs. 33 (5.099), $P < 0.05$]. In patients with a short time between drug and disease onset (<4.2 years), fibrosis and p53 positively correlated ($r = 0.76$, $P < 0.05$), and in those with late onset disease (>4.2 years), cellular abnormalities and p53 trended to a positive correlation and cardiotoxicity risk scores and p53 positively correlated ($r = 0.95$, $P < 0.05$). A year after biopsy, the short-term group had significant recovery of ejection fraction compared with the long-term group ($P < 0.05$). The CTRCD group had a significantly worse overall survival prognosis than the control group [hazard ratio 7.61 (95% confidence interval 1.30–44.6), $P < 0.05$]. Autopsy cases with cancer treatment also had a high grade of histopathological changes, with even more severe changes in patients with cardiac dysfunction, and had increased p53 and H3K27ac expression levels, compared with controls. H-scores of p53 and H3K27ac showed a positive correlation in the CTRCD group in biopsy cases ($r = 0.62$, $P < 0.05$) and a positive correlation in autopsy cases.

Conclusions Our results indicate distinct morphological characteristics in myocardial histopathology associated with CTRCD. p53 and H3K27ac histone modification could be sensitive markers of CTRCD and suggest a mechanistic involvement of epigenetic changes.

Keywords endomyocardial biopsy; epigenetics; histone acetylation; oncocardiology; p53

Received: 30 November 2021; Revised: 26 April 2022; Accepted: 9 June 2022
**Correspondence to: Kenji Onoue, Department of Cardiovascular Medicine, Nara Medical University, 840 Shijo, Kashihara, Nara, 634-8522, Japan. TEL: +81-744-22-3051; FAX: +81-744-22-9726. Email: konoue@naramed-u.ac.jp*
Kinta Hatakeyama, Department of Pathology, National Cerebral and Cardiovascular Center, 6-1 Kishibe-Shimmachi, Suita, Osaka, 564-8565, Japan. Tel: +81-6-6170-1070 (ext.31222); Fax: +81-6-6170-1956. Email: kpathol@naramed-u.ac.jp

Introduction

In recent years, progress in cancer treatment has dramatically improved the long-term survival rate of cancer patients.[1] However, cardiotoxicity related to such treatment is frequently reported, particularly linked to anthracycline, molecularly targeted drugs, and immune checkpoint inhibitors.[2–6] Cancer therapy-related cardiac dysfunction (CTRCD) has become the second leading cause of cancer-related mortality.[7–9]

The causes of CTRCD may be related to oxidative stress, endoplasmic reticulum stress, and mitochondrial dysfunction, but the mechanistic details are not known.[2–5,10] Recently, heart failure has been linked to increased expression of p53, epigenetic changes such as histone modifications, and DNA methylation,[11] but the relationship of these factors with CTRCD is not clear.

In some cases, asymptomatic cardiac dysfunction progresses over a prolonged period of time after cancer treatments and is diagnosed as CTRCD only after symptoms appear. A multi-hit hypothesis established for the pathogenesis of CTRCD suggests contributing factors occurring later may precipitate cardiac dysfunction.[4,12] A cardiotoxicity risk score (CRS) has been proposed to evaluate CTRCD risk, incorporating medication and patient-related risk factors (e.g. sex, age, history of high blood pressure, diabetes, and radiation therapy).[13–15] However, its usefulness has been little investigated in a clinical setting.

In this study, we characterized the short-term to long-term histopathology of CTRCD and evaluated the association between histological parameters and medication-related and patient-related risk factors. We hypothesized that immunohistological staining for p53 and acetylation of lysine 27 on histone H3 (H3K27ac) could be novel markers of cardiac dysfunction in cancer patients.

Methods

Materials

Specimens archived in the Pathology Department of Nara Medical University, Japan, were retrieved to evaluate their histopathological changes in correlation with recorded clinical features of cardiotoxicity. This study included several cohorts. First, we examined 13 endomyocardial biopsy specimens stored between January 2010 and December 2019 from the left ventricles of patients who developed CTRCD after anticancer treatments (*Table 1*). CTRCD was defined based on a reduction in left ventricular ejection fraction (LVEF) of >10% from baseline to a value below 53%.[16] Second, we evaluated histopathological changes in the myocardium of 35 autopsied patients who died after cancer treatments at Nara Medical University from 2010 to 2020. These patients were diagnosed with oesophageal cancer (n = 16), leukaemia (n = 7), or lymphoma (n = 12) (*Table 2*). Third, we included controls: 10 biopsy samples with no history of cancer and mild cardiac dysfunction and 9 autopsy cases of non-cardiac death without cancer. In the biopsy control cases, biopsies were performed on suspected cases of dilated cardiomyopathy (DCM), and patients were diagnosed as normal or having mild DCM. For all

Table 1 Clinical characteristics of patients who developed chemotherapy-related cardiac dysfunction (CTRCD) after anticancer treatments and underwent endomyocardial biopsy

Case	Age/sex	Tumour	Chemotherapy	CRS	Time from chemotherapy to onset of CTRCD (years)
1	44/F	Breast cancer	FEC, Herceptin, docetaxel	6	0.5
2	61/M	Synovial sarcoma	Pazopanib, doxorubicin	5	0.5
3	74/M	Lung cancer	Crizotinib	3	0.5
4	51/F	Uterine cancer	Paclitaxel, carboplatin, anaphylaxis, doxorubicin, cisplatin	7	0.5
5	68/F	Breast cancer	Herceptin, TS-1	6	1
6	67/F	Breast and stomach cancer	Epirubicin, cyclophosphamide, 5-FU, vinorelbine	7	1
7	58/F	ALL	R-CHOP, MTX, Ara-C	7	1
8	70/F	AML	Doxorubicin, cyclophosphamide, oxaliplatin, paclitaxel, Ara-C	9	1.2
9	45/F	Ovarian cancer	Paclitaxel, bevacizumab, doxorubicin	5	7
10	42/F	Uterine cancer	TC	3	9
11	75/M	DLBCL	R-CHOP, CHASER	8	10
12	68/M	Stomach cancer	TS-1, CDDP, 5-FU	2	10
13	68/F	Breast cancer	FEC, cisplatin, irinotecan, TS-1,bevacizumab	8	12

Abbreviations: 5-FU, 5-fluorouracil; ALL, acute lymphocytic leukaemia; AML, acute myelogenous leukaemia; Ara-C, cytarabine; CDDP, cisplatin; CHASER, chemotherapy regimen including cyclophosphamide, Ara-C, etoposide, dexamethasone, granulocyte-colony stimulating factor and rituximab; CRS, cardiotoxicity risk score; CTRCD, chemotherapy-related cardiac dysfunction; DLBCL, diffuse large B-cell lymphoma; F, female; FEC, chemotherapy regimen including 5-FU, doxorubicin and cyclophosphamide; M, male; MTX, methotrexate; R-CHOP, chemotherapy regimen including rituximab, cyclophosphamide, doxorubicin, vincristine and prednisolone; TC, chemotherapy regimen including carboplatin and paclitaxel; TS-1, tegafur/gimeracil/oteracil potassium.

Table 2 Clinical characteristics of cases autopsied after cancer treatment

Case	Age/Sex	Tumour	Chemotherapy	Other therapies	CRS	Heart failure symptoms
1	66/M	Oesophageal cancer	Cisplatin, 5-FU	RT	1	Cardiac dysfunction (details unknown), arrhythmia
2	83/M	Oesophageal cancer	—	Op	1	Cardiac dysfunction (EF, 60%; BNP, 236), pericardial effusion
3	90/M	Oesophageal cancer	—	RT	3	—
4	81/M	Oesophageal cancer	—	RT	5	—
5	75/M	Oesophageal cancer	NDP, cisplatin, 5-FU, TS-1	RT	4	—
6	86/M	Oesophageal cancer	-	Op	0	—
7	64/M	Oesophageal cancer	+ (details unknown)	RT	Unknown	—
8	63/M	Oesophageal cancer	Cisplatin, 5-FU	Op, RT	Unknown	—
9	66/M	Oesophageal cancer	-	RT	Unknown	—
10	42/M	Oesophageal cancer	+ (details unknown)	RT	Unknown	—
11	42/F	Oesophageal cancer	Cisplatin, 5-FU	RT	2	—
12	67/M	Oesophageal cancer	Cisplatin, 5-FU, cetuximab	RT	5	Cardiac dysfunction (EF54%, BNP, 133)
13	84/M	Oesophageal cancer	—	—	4	—
14	41/M	Oesophageal cancer	Cisplatin, 5-FU, docetaxel	RT	2	—
15	84/M	Oesophageal cancer	—	—	3	—
16	64/M	Oesophageal cancer	Cisplatin, 5-FU, paclitaxel	RT	2	—
17	49/M	AML	Idamycin, ara-C, MIT, DEX	—	4	Cardiac dysfunction (BNP, 50.1)
18	74/M	AML	Idamycin, ATRA, ara-C, MIT, trisenox, etoposide, DNR	—	10	Cardiac dysfunction (EF, 61%; BNP, 678)
19	61/M	ATL	Doxorubicin, vincristine, cyclophosphamide, ranimustine, vindesin, etoposide, carboplatin	—	11	—
20	76/M	AML	Aclarubicin, ara-C	—	10	—
21	60/M	CML	—	—	2	—
22	85/M	AML	Ara-C, aclarubicin, MAG	—	8	—
23	48/F	AML	CVAD, MTX	—	8	—
24	87/M	DLBCL	—	—	2	—
25	36/F	DLBCL	—	—	0	—
26	48/M	DLBCL	Cyclophosphamide, rituximab, etoposide, ara-C, pirarubicin, vincristine	—	0	—
27	75/M	IVLBCL	—	—	Unknown	—
28	60/F	DLBCL	Cyclophosphamide, doxorubicin, MTX, ara-C, vincristine	—	Unknown	—
29	74/F	DLBCL	Cyclophosphamide, doxorubicin, vincristine, rituximab, etoposide	—	11	Cardiac dysfunction (details unknown)
30	71/F	DLBCL	THP-COP	—	Unknown	—
31	87/F	MCL	THP-COP	—	Unknown	—
32	57/M	NK/T-cell lymphoma	+ (details unknown)	—	Unknown	—
33	70/M	ML	+ (details unknown)	-	Unknown	—
34	85/M	ML	+ (details unknown)	-	Unknown	—
35	70/M	FL	Bendamustine, rituximab	-	Unknown	Cardiac dysfunction (EF, 30%; BNP, 1000)

Abbreviations: 5-FU, 5-fluorouracil; AML, acute myelogenous leukaemia; AML, acute myelogenous leukaemia; and 5-fluorouracil; Ara-C, cytarabine; ATL, adult T-cell leukaemia; BNP, B-type natriuretic peptide (pg/mL); CDDP, cisplatin; CHASER, chemotherapy regimen including cyclophosphamide, ara-C, etoposide, dexamethasone, granulocyte-colony stimulating factor, and rituximab; CML, chronic myelogenous leukaemia; CRS, cardiotoxicity risk score; CTRCD, chemotherapy-related cardiac dysfunction; CVAD, chemotherapy regimen including cyclophosphamide, doxorubisin, vincristine, and cytarabine; DLBCL, diffuse large B-cell lymphoma; DNR, daunomycin; F, female; FEC, chemotherapy regimen including 5-fluorouracil, doxorubicin, and cyclophosphamide; FL, follicular lymphoma; IVLBCL, intravascular large B-cell lymphoma; M, male; MCL, mantle cell lymphoma; MIT, mitoxantrone; ML, malignant lymphoma; MTX, methotrexate; NK/T-cell lymphoma, natural killer T-cell lymphoma; Op, operation; R-CHOP, chemotherapy regimen including rituximab, cyclophosphamide, doxorubicin, vincristine, and prednisolone; RT, radiation; THP-COP, chemotherapy regimen including rituximab, pirarubicin, cyclophosphamide, vincristine, prednisolone; TS-1, tegafur/gimeracil/oteracil potassium.

autopsy cases, the anterior to posterior walls of the post-mortem left ventricle were examined histologically as described previously.[17]

All specimens were fixed in 10% neutral buffered formalin and embedded in paraffin. These tissue sections were stained with haematoxylin-eosin and Mallory-azan stains for morphological analysis, and serial sections were stained with primary antibodies for immunohistochemical analysis (as described in Immunohistological evaluation section).

Written informed consent was obtained from patients and bereaved families in all biopsy and autopsy cases, respectively. This study was approved by the Human Investigation Review Committee of Nara Medical University (No. 2565) and conformed to the principles outlined in the Declaration of Helsinki.[18]

For all biopsy and autopsy cases, medication and patient-related risk factors were used to calculate the CRS.[13] In this scoring system, each of the following patient-related risk factors scores one point: previous radiotherapy and treatment with anthracyclines, coronary artery disease or heart failure, diabetes mellitus, hypertension, female gender, and age $<$15 years or $>$65 years. Medications contribute to the score as follows: one point for bevacizumab or imatinib, two points for docetaxel, and four points for anthracycline, trastuzumab, or cyclophosphamide. Moreover, CTRCD can be classified into Type 1 and Type 2 based on the type of anticancer drug: Type 1 is caused by anthracyclines and cyclophosphamide, whereas Type 2 is caused by trastuzumab and bevacizumab.

Histological evaluation and scoring

All tissue sections were scored for their extent of fibrosis (interstitial and replacement) and the severity of cardiomyocyte changes (nuclear atypia, disarrangement, sarcoplasmic rarefaction, cardiomyocyte tapering, and cytoplasmic vacuolation) by two evaluators (CT and KH). Fibrosis was graded as follows: 0, absent; 1, $<$5%; 2, 5–10%; 3, 10–20%; and 4, $>$20% of the myocardium. Changes in cardiomyocytes under light microscopy were graded as follows: 0, absent; 1, mild; 2, moderate; 3, severe; and 4, extremely severe.

Immunohistological evaluation

Immunostaining was performed using antibodies against p53 (Leica, NCL-L-p53-DO7, 1:800 dilution), H3K27ac (Gene Tex, GTX128944, 1:1000 dilution), histone acetyltransferase 1 (HAT1, Santa Cruz, sc-390562, 1:50 dilution), p300 (Santa Cruz, sc-48343, 1:30 dilution), and myocyte enhancer factor-2(MEF2A, Santa Cruz, sc-17785, 1:5000 dilution) on an automated immunohistochemistry stainer (Bond Max, Leica Biosystems). Normal mouse and rabbit sera were used for negative control stains instead of p53, H3K27ac, HAT1, p300, and MEF2A antibodies, respectively.

For the immunohistochemical evaluation, the histological score (H-score) was calculated by determining the staining intensity and coverage as previously reported.[19,20] Briefly, the percentage of positive nuclei (0–100%) was multiplied by the immunohistochemical intensity (Score 0: negative; Score 1–3: positive, with a higher score representing more intense staining). In biopsy cases, all cardiomyocytes were evaluated by this scoring system, and in autopsy cases, all cardiomyocytes in 10 high-power fields were evaluated.

Prognostic evaluation

For survival, we recorded survival times of all patients from the time of biopsy to the year 2021. For cardiac function in CTRCD patients, the LVEF was evaluated 1 year after biopsy.

Statistical analysis

Statistical analyses were performed using GraphPad Prism (version 8.4.3). Data are presented as numbers with percentages or means with standard error. Quantitative variables between two groups were compared using Student's *t* test or the Mann–Whitney *U* test as appropriate. Correlations between the changes in histopathological features were assessed using Spearman's correlation coefficients. All survival times were calculated using Kaplan–Meier estimates and compared using the Wilcoxon test. A two-way ANOVA was used to compare the 1 year change in LVEF. All tests were two-sided, and *P* values of $<$0.05 were considered significant.

Results

Characteristics of biopsy patients and autopsy cases

Of the 13 biopsy cases with CTRCD, 4 patients had breast cancer, 2 had stomach cancer (including a patient who had both), 2 had uterine cancer, and the others had synovial sarcoma, lung cancer, acute lymphocytic leukaemia, acute myelogenous leukaemia, ovarian cancer, and malignant lymphoma (*Table 1*). Among the included patients, 10 (76.9%) received high-risk chemotherapies, like anthracyclines, trastuzumab, and cyclophosphamide. Of the patients, 9 (69.2%) received Type 1 drugs (two of which also used Type 2 drugs), with cumulative anthracycline doses of over 400 mg/m^2 administered to all patients, whereas 1 patient received Type 2 drugs. The CRS for biopsy CTRCD cases were also presented in *Table 1*. The average CRS was 5.8 and ranged from 2 to 9.

Detailed patient backgrounds, including medical history and laboratory values, are summarized in Supporting information *Table S1* and controls in *Table S2*, and a comparison with the control group is shown in *Table S3*. Compared with the control group, the CTRCD group had significantly fewer men, lower incidence of hypertension history, lower LVEF, and higher levels of B-type natriuretic peptide (BNP).

Cancer therapy-related cardiac dysfunction was diagnosed 0.5 to 12 years after the initiation of chemotherapy (*Table 1*). We divided the patients into two groups based on the average time to onset (4.2 years): Those with dysfunction occurring in the relative short-term (<4.2 years, n = 8) and those with dysfunction in the long-term (>4.2 years, n = 5). The medical history and laboratory values were compared between the two groups, but there were no obvious differences (*Table S4*).

In autopsy cases, the treatment varied depending on the case, including surgery, chemotherapy and radiation therapy. Patients with oesophageal cancer were treated with operation, radiation, and chemotherapy [5-fluorouracil (5-FU) and cisplatin (CDDP)]. Patients with lymphoma were treated with rituximab plus cyclophosphamide, doxorubicin, vincristine, and prednisone (R-CHOP). For patients with leukaemia, cytarabine, mitoxantrone, and aclarubicin, a kind of anthracycline, were often used. Of the 35 patients in this cohort, 7 developed cardiac dysfunctions, as described in *Table 2* [based on their ejection fraction (EF) and BNP]. Detailed patient autopsy backgrounds, including medical history and laboratory values, are summarized in *Table S5*.

Histopathological changes in fibrosis and cardiomyocytes in cases with or without CTRCD

Histopathological changes were scored as described in the Methods (*Figure S1G*). In the biopsy cases, all histopathological changes were significantly more severe in the CTRCD group than the control (*Figure 1A–G*). The following mean (SE) scores were recorded in the CTRCD group and the control group, respectively: interstitial fibrosis 2.2 (0.359) vs. 0.3 (0.153), $P < 0.001$; replacement fibrosis 1.8 (0.629) vs. 0.1 (0.100), $P < 0.05$; nuclear atypia 2.0 (0.211) vs. 0.6 (0.163), $P < 0.001$; disarrangement 2.1 (0.379) vs. 0.2 (0.133), $P < 0.001$; sarcoplasmic rarefaction 2.1 (0.407) vs. 0.5 (0.167), $P < 0.01$; cardiomyocyte tapering 1.9 (0.277) vs. 0.2 (0.133), $P < 0.001$; and cytoplasmic vacuolation 1.5 (0.307) vs. 0.7 (0.213), $P < 0.05$. Autopsy cases also showed significant histopathological changes compared with the controls, similar to the biopsy cases (*Figure S2*).

Figure 1 Evaluation of histological findings in control and cancer therapy-related cardiac dysfunction (CTRCD) cases scored on a scale of 0–4, with a higher score representing a more severe change. (A,B) All scores of fibrosis and (C–G) cardiomyocyte changes were significantly higher in the CTRCD group than the control group. Student's *t* or Mann–Whitney *U* tests were performed as appropriate. (A) Interstitial fibrosis; (B) Replacement fibrosis; (C) Nuclear atypia; (D) disarrangement; (E) Sarcoplasmic rarefaction; (F) Cardiomyocyte tapering; (G) Cytoplasmic vacuolation.

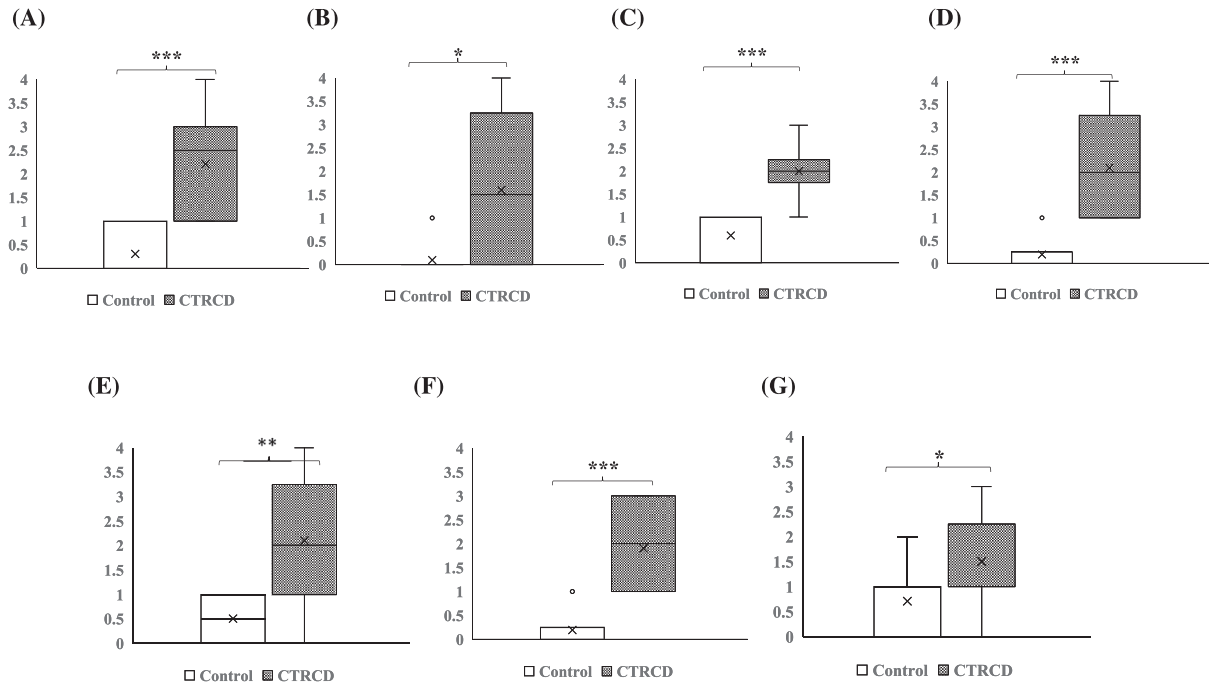

H-scores of p53 and H3K27ac in biopsy cases

The expression levels of p53 and H3K27ac were evaluated by immunohistochemistry in biopsy cases and analysed by H-score, as described in the Methods section (*Figure S3*). Although the nuclei in some vascular endothelial cells and stromal cells stained positive for p53 and H3K27ac, most positively stained cells were cardiomyocytes, so only cardiomyocytes were counted in the score. For p53, the H-score was significantly higher in the CTRCD group than the control group [63 (9.109) vs. 33 (5.099), respectively, $P < 0.05$] (*Figure 2A*). However, for H3K27ac, the H-score did not differ between CTRCD and control [139 (11.77) vs. 120 (11.57), respectively, $P = 0.36$] (*Figure 2B*).

Positive correlation between p53 and H3K27ac in biopsy cases with CTRCD

In the CTRCD biopsy cases, there was a positive correlation between the H-scores of p53 and H3K27ac ($r = 0.62$, $P < 0.05$) (*Figure 2C*). In contrast, in the control cases, there was no significant correlation ($r = 0.53$, $P = 0.11$).

Changes in histopathological features depending on the time to onset

As described in the Methods section, the CTRCD biopsy cases were divided into the following two groups according to the time from drug administration to CTRCD onset: short-term (<4.2 years) and long-term (>4.2 years) group. Thereafter, CRS scores and histological and immunohistochemical changes were compared.

The total score of CRS was calculated by adding the medication score and patient-related risk factor score. No differences in the total score of CRS [6.3 (1.639) vs. 5.2 (2.482), respectively, $P = 0.42$], medication score [3.5 (1.323) vs. 2.4 (1.960), respectively, $P = 0.29$] or patient-related risk factor score [2.75 (1.090) vs. 2.80 (1.166), respectively, $P = 0.94$] was observed between the short-term and long-term groups (*Figure S4A–C*).

Regarding histological findings, we examined the total score of fibrosis [4.1 (2.260) vs. 4.6 (3.382), respectively, $P = 0.79$] and the total cardiomyocyte change score [8.9 (3.551) vs. 10.0 (3.286), respectively, $P = 0.61$], but no clear differences were found (*Figure S4D,E*). We also examined p53 as an immunohistochemical finding and found no difference [72.4 (28.41) vs. 47.3 (30.03), respectively, $P = 0.19$]

Figure 2 Histological scores (H-scores) for p53 and H3K27ac immunohistochemistry in control and cancer therapy-related cardiac dysfunction (CTRCD) cases, and correlation between histological scores (H-scores) for p53 and H3K27ac. (A) The H-score for p53 was significantly higher in CTRCD cases than in the control cases. (B) The H-score for H3K27ac did not differ between the two groups. Student's *t* test, $*P < 0.05$. (C) In CTRCD cases, there was a positive correlation between p53 and H3K27ac (solid line). In control cases, there was no obvious correlation (dotted line). Spearman correlations were performed.

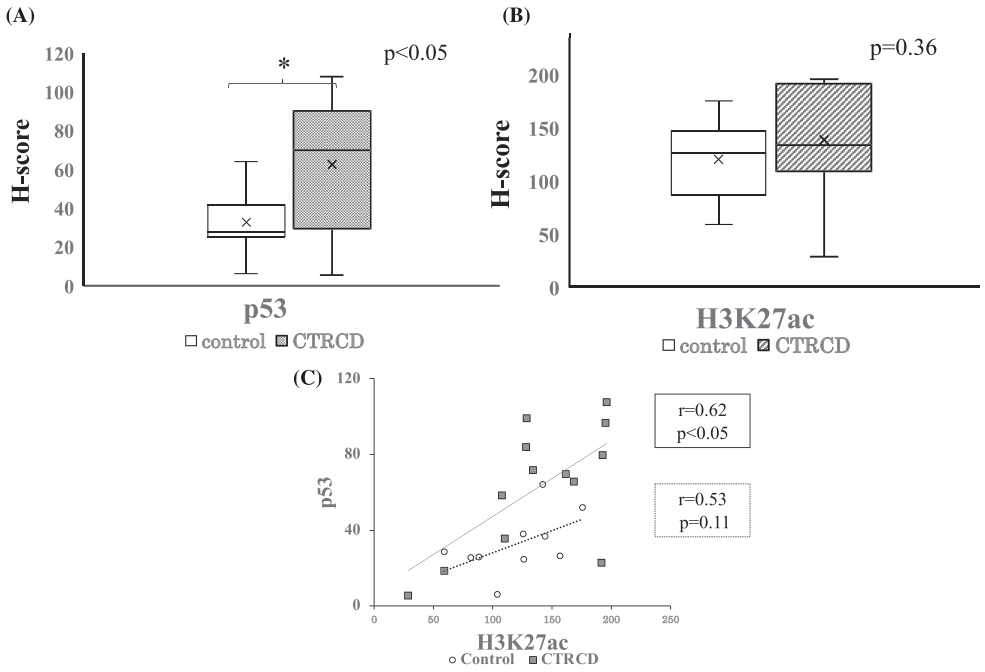

(*Figure S4F*). However, the short-term group had significantly higher H3K27ac expression compared with the long-term group [164.6 (32.83) vs. 97.1 (47.68), respectively, $P = 0.02$] and the control group [164.6 (32.83) vs. 120.3 (34.71), respectively, $P = 0.02$] (*Figure S4G*).

Relationship among histopathological features depending on time to onset of disease

This study also examined the relationship between histological and immunohistochemical changes as well as CRS scores in the short-term and long-term groups. In the short-term group, there was a positive correlation between the p53 H-score and the total fibrosis score ($r = 0.76$, $P < 0.05$) (*Figure 3A*). In the long-term group, the p53 H-score trended towards a positive correlation with the total cardiomyocyte change score (*Figure 3B*), and positively correlated with CRS ($r = 0.96$, $P < 0.05$) (*Figure 3C*).

Comparison between Type 1 and Type 2 CTRCD

Among the present biopsy cases, nine had Type 1 CTRCD (two of which also used Type 2 drugs) and one had Type 2 CTRCD. Among those with Type 1 CTRCD, six were in the short-term group and three were in the long-term group. The only Type 2 CTRCD case was in the short-term group. No significant difference in CRS scores were noted between the two groups (*Figure S5A*).

Earlier reports suggested that Type 1 CTRCD cases exhibited histological changes, such as cardiomyocyte necrosis, with dose dependency and irreversibility but that Type 2 cases showed no morphological changes, were dose independent, and were reversible.[13,19,21] Owing to the small number of cases, determining statistically significant differences between the two types was not possible. In the current study, histological changes were observed in both Type 1 and Type 2 CTRCD cases, although no obvious differences were noted (*Figure S5B,C*; H-scores for p53 and H3K27ac were also as shown in *Figure S5D,E*).

Furthermore, recent reports have shown that Type 2 cardiotoxicity was irreversible and that Type 1 cardiotoxicity improves EF with early therapeutic intervention.[19,22–24] However, both Type 1 and Type 2 CTRCD cases were reversible in this study (*Figure S5F*).

Although some of the details of the autopsy cases were unknown, Type 1 CTRCD accounted for 11 cases, with 6 having leukaemia and 5 having lymphoma. In contrast, clear

Figure 3 Correlations between histopathological features or cardiotoxicity risk score (CRS) and p53 histological scores (H-scores) according to time from drug administration to cancer therapy-related cardiac dysfunction (CTRCD) onset (short term, <4.2 years; and long-term, >4.2 years). (A) In the short-term group, there was a positive correlation between the total fibrosis score (interstitial and replacement) and the p53 H-score. (B,C) In the long-term group, the p53 H-score (B) trended towards a positive correlation with the total score of cardiomyocyte changes (nuclear atypia, disarrangement, rarefaction, tapering, and vacuolation), and (C) positively correlated with CRS. Spearman correlations were performed.

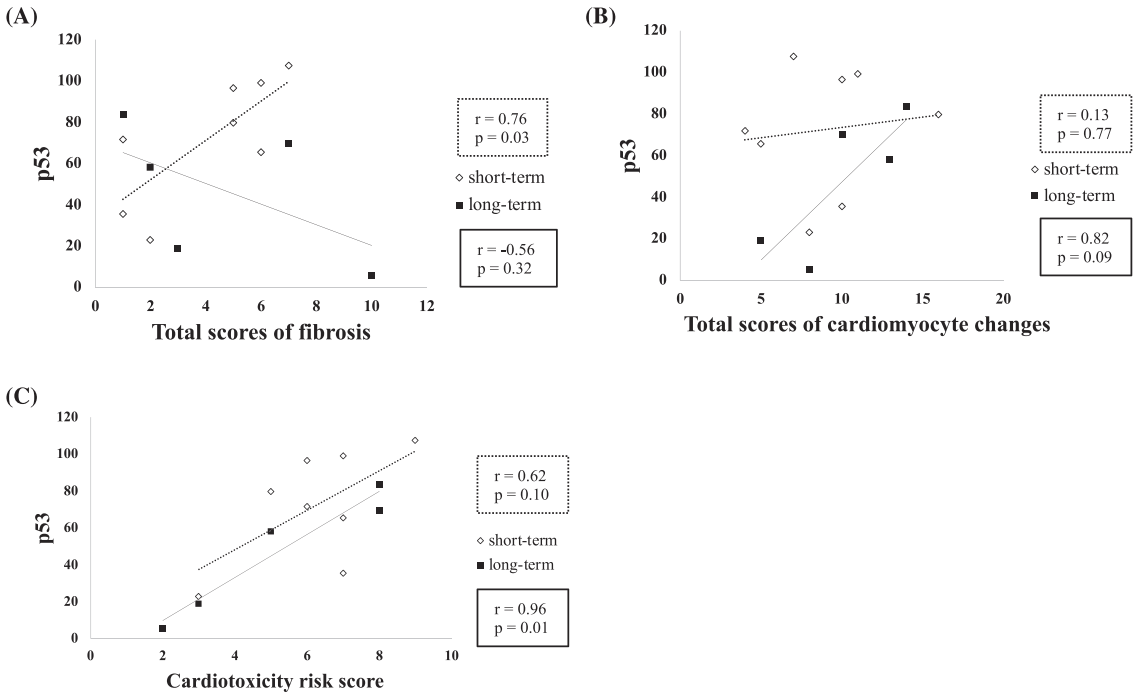

history of Type 2 drug use could not be determined, making it difficult to compare them in autopsy cases.

Prognostic evaluation

In the CTRCD biopsy cases, we were able to follow-up survival for up to 6 years. When the overall survival of the controls and the CTRCD group was compared, the CTRCD group had a significantly worse overall survival prognosis than the control group [HR 7.61, 95% confidence interval (CI) 1.30–44.6, P = 0.03] (*Figure 4A*).

In the CTRCD cases, there was no clear difference in overall survival prognosis between the groups with long-term and short-term disease onset (HR 2.76, 95% CI 0.38–19.9, P = 0.44) (*Figure 4B*). However, the LVEF recovery 1 year after the time of biopsy was significantly better in the short-term group than in the long-term group (P = 0.03) (*Figure 4C*).

We also divided the CTRCD group into two groups based on the mean values of CRS, p53 H-score, fibrosis, and cardiomyocyte change scores at the time of biopsy. The group with values higher and lower than mean value was determined as the high and low group, respectively. However, no clear difference in LVEF recovery was observed based on either parameter (*Figure S6*).

Histopathological changes in the autopsy cases with or without CTRCD

In the autopsy cases, the p53 and H3K27ac H-scores in the patients treated with cancer therapy were compared with those of the control cases (*Figure 5A,B*). The p53 and H3K27ac (H-scores) were significantly increased in cases where patients died after treatment of various tumours compared with control, in all cancer types (oesophageal cancer, leukaemia, and lymphoma). When these groups were analysed separately for correlations between p53 and H3K27ac H-scores, all cancer types showed a positive correlation (oesophageal cancer, n = 16) or trend to a positive correlation (lymphoma, n = 12; and leukaemia, n = 7), but correlation coefficients and slopes differed from tumour to tumour, with the highest correlation coefficient in the oesophageal cancer group (*Figure 5C*). The autopsy cancer treatment cases with cardiac dysfunction had significantly higher H-scores for p53 and H3K27ac than those without cardiac dysfunction (*Figure 6A,B*).

Immunostaining for epigenetic transcriptional activators such as MEF2A, histone acetyltransferase p300, and HAT1, which are transcriptional regulators of myocardium associated with H3K27ac, was also performed and calculated by H-score, as described in the Methods section (*Figure S7*). The H-scores of HAT1 were significantly increased in cases

Figure 4 Kaplan–Meier analysis for the control and the cancer therapy-related cardiac dysfunction (CTRCD) group and comparison of left ventricular ejection fraction (LVEF) recovery based on time to disease onset. (A) The CTRCD group had a significant decrease in survival compared with control, and (B) no clear difference in survival was observed between the short-term and long-term groups. (C) A comparison of LVEF at the time of biopsy and 1 year later between the short-term and long-term groups showed that ejection fraction (EF) recovery was improved in the short-term group based on the two-way analysis of variance analysis.

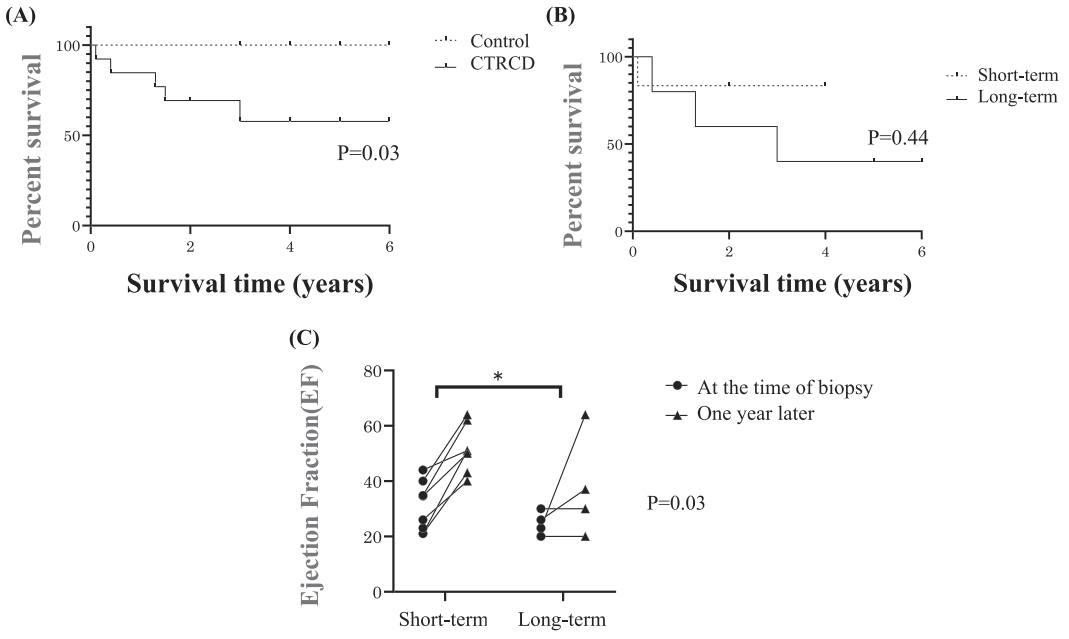

Figure 5 Histological scores (H-scores) for p53 and H3K27ac and correlations between histological scores (H-scores) for H3K27ac and p53 in autopsy samples from patients on cancer treatment (divided into groups based on cancer type) and controls. (A, B) The H-scores for p53 and H3K27ac were significantly higher in cases where patients died after treatment for various tumours than in the controls. Student's *t* test; $*P < 0.05$, $**P < 0.01$, $***P < 0.001$ vs. control. (C) A positive correlation and trend to positive correlation between H3K27ac and p53 were found in oesophageal cancer and lymphoma, respectively. Spearman correlations were performed.

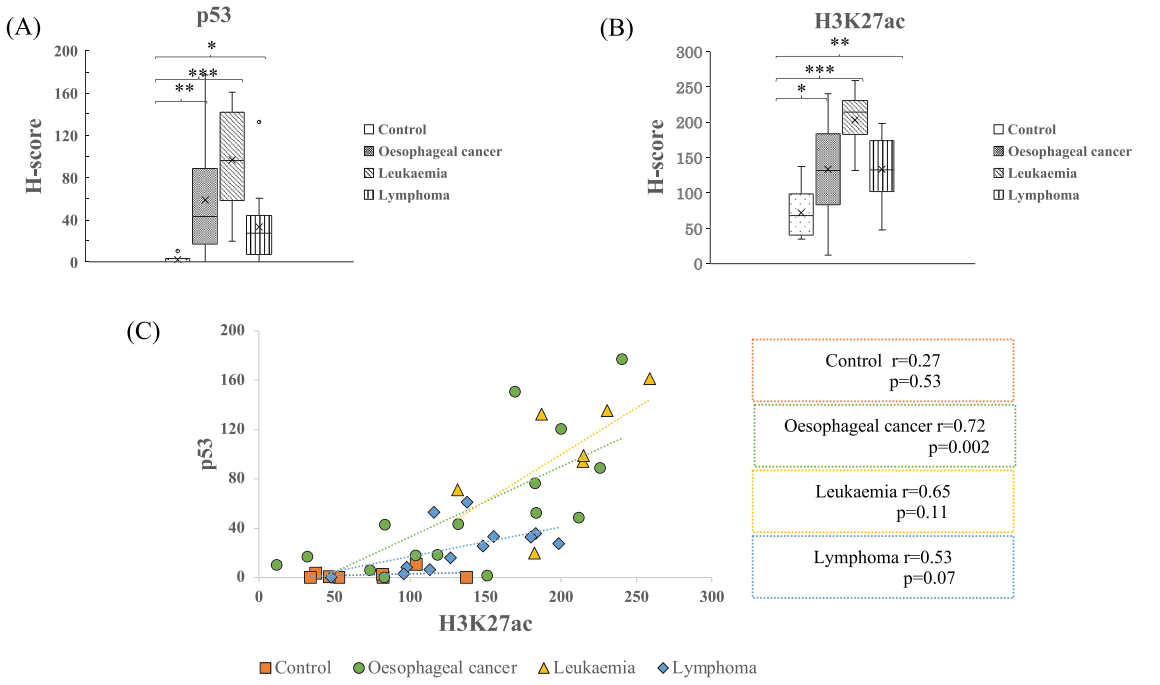

Figure 6 Histological scores (H-scores) of p53 and H3K27ac in the cancer treatment autopsy cases with and without cardiac dysfunction. (A,B) H-scores of p53 and H3K27ac were significantly higher in cases with cardiac dysfunction than those without. Student's *t* test, $*P < 0.05$, $**P < 0.01$.

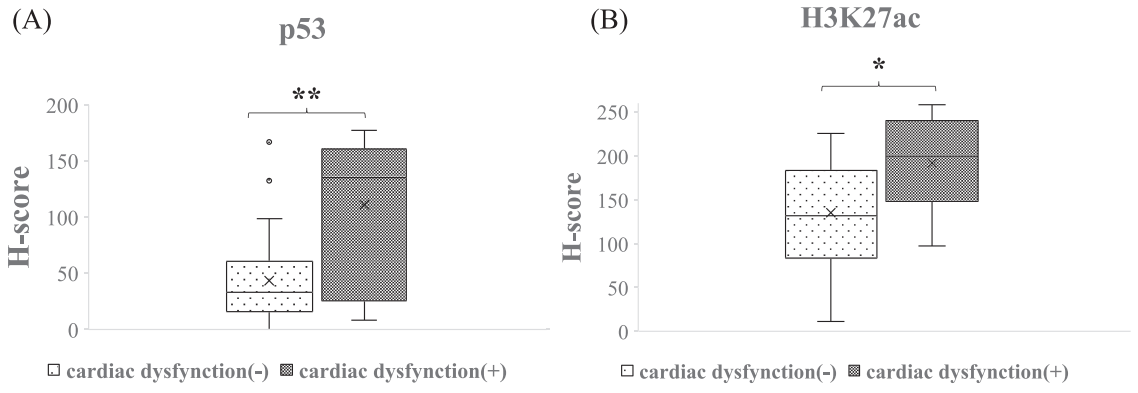

where patients died after treatment of various tumours compared with control, in all cancer types (*Figure S8A*). Significant positive correlation was found between HAT1 and H3K27ac ($r = 0.72$, $P = 0.00001$) and p53 ($r = 0.63$, $P = 0.00001$) in total autopsy cases. In each autopsy case, a significant positive correlation was found between oesophageal cancer ($r = 0.72$, $P = 0.002$) and leukaemia ($r = 0.79$, $P = 0.04$) for HAT1 and H3K27ac and oesophageal cancer ($r = 0.66$, $P = 0.005$) for HAT1 and p53 (*Figure S8B,C*). No clear correlation was found with MEF2A or p300 (*Figures S9* and *S10*).

We examined the time from death to autopsy and found no differences between cancers. No correlation was observed between immunohistological results, such as p53 or H3K27ac, and time from death to autopsy (*Figure S11*).

Discussion

In this study, we found a higher grade of cardiomyocyte changes and fibrosis in endomyocardial biopsy samples from CTRCD cases than from controls regardless of the type of cancer drug, and the immunoreactivity of the p53 protein was significantly higher in CTRCD cases. Similar histological and immunohistochemical findings were observed in the myocardium of autopsied cancer cases, especially in those with cardiac dysfunction. In addition, there was a significant positive correlation between the immunoreactivity of p53 and H3K27ac in cancer patients with CTRCD. Furthermore, in the group of biopsy cases with CTRCD developing late after treatment (>4.2 years), cardiomyocyte changes and CRS positively correlated with p53. These results suggest that the changes in cardiomyocytes and increased expression of p53 in CTRCD cases are partly mediated by altered epigenetic modifications.

p53, a DNA binding transcription factor, is famous for its tumour-suppressive effects. Recently, it has been found to be expressed in response to various stresses such as hypoxia, endoplasmic reticulum stress, and oxidative stress, leading to DNA repair, cell cycle regulation, senescence and apoptosis, and is up-regulated in the failing human heart.[16] In the present study, we detected increased expression of p53 in biopsies from patients with CTRCD, not only in those taking anthracyclines but also other cancer drugs. In autopsy samples from a variety of cancer patients, p53 expression was increased even in the absence of heart failure, and it was even higher in cases with heart failure symptoms (refer to *Figure 6*). These results suggest that increased p53 expression is associated with myocardial damage; it may be a marker for the development of cardiac dysfunction even in the absence of symptoms.

Heart failure is a multifactorial disease linked to a history of hypertension, diabetes mellitus, dyslipidaemia, smoking, and alcohol consumption, in addition to genetic background,[8,25–27] and epigenetic changes or gene mutations have recently been suggested as a pathogenic mechanism.[28] H3K27ac, an epigenetic modification to histone H3 associated with enhancer activity, is increased in chronic heart failure, and p53 is involved in the regulation of gene expression through recognizing the modification changes of H3K27ac.[8,20,29–32] In this study, we found a significant positive correlation between the immunoreactivity of p53 and H3K27ac in CTRCD. We also found a positive correlation between H3K27ac and HAT1 expression, a histone acetyltransferase. In addition, in a group of patients who developed CTRCD long after treatment, p53 expression positively correlated with more severe cardiomyocyte changes and CRS. We hypothesize that environmental factors associated with CRS may accumulate and lead to the development of CTRCD when they reach a certain threshold, and that this accumulation factor may be an epigenetic modification in cardiomyocytes. It is also possible that histone modifications may lead to changes in gene expression when then contributes to the eventual development of heart failure. Our future studies will focus on elucidating the mechanism underlying the mutual regulation of the expression of p53 and H3K27ac.

However, in a group of patients with a decline in cardiac function only a short time after treatment, there was no association between p53 and CRS or other environmental factors. We hypothesize that the cardiac dysfunction seen in this group might be directly related to individual genetic factors. There are several genes known to be associated with heart failure, and TTN gene mutations are one of the causes of CTRCD in Caucasians.[33–35] DCM patients with mutations in the TTN gene had a significant recovery in LVEF after medical therapy compared with a group with other mutations,[36] similar to our finding that the early onset CRTCD group had significantly better LVEF recovery than the late onset CRTCD group. We therefore further hypothesize that the genetic factors contributing to CRTCD in the early onset group could include mutations to the TTN gene.

Overall, we considered two major factors to be responsible for the development of CTRCD in our cohort: genetic factors in the short term and environmental factors over a longer period. These factors may interact; based on the individual genetic factors, the burden of various environmental factors may accumulate in the form of epigenetic modification changes. The administration of anticancer drugs may then cause CTRCD to develop more quickly in those patients with a higher existing burden of contributing factors. Genetic factors may therefore play a major role in CTRCD cases observed in the early stage after treatment, and genetic and epigenetic analysis will be a future area of study to identify at-risk patients.

Limitation

This study has some limitations that should be taken into account. Many of the autopsy cases in this study were not evaluated for CTRCD by cardiologists; they are essentially just patients with a history of cancer treatment. The sample size of the CTRCD cohort was extremely small, which made it difficult to conduct an analysis based on type of medication, including Type 1 and Type 2 drugs. Compared with controls, the CTRCD group had significantly fewer men, lower incidence of history of hypertension, lower LVEF, and higher levels of BNP. To elucidate the mechanisms of cardiac dysfunction, evaluating not only myocardial cells but also blood vessels and surrounding connective tissues that make up myocardial tissue is imperative. However, the present study was limited to cardiomyocytes.

Conclusions

This study revealed morphological characteristics in myocardial histopathology associated with CTRCD, including fibrosis and cardiomyocyte changes. The expression of p53 and H3K27ac modification could be a sensitive marker of cardiac dysfunction, suggesting the involvement of epigenetic modification as a cause of CTRCD.

Acknowledgements

We thank Mr. Lota Liu and Mrs. Masako Nakata for their technical assistance.

Conflict of interest

None declared

Funding

This study was supported in part by Grants-in-Aid for Scientific Research in Japan (grant no, 21K06941) from the Ministry of Education, Culture, Sport, Science, and Technology, Japan.

Supporting information

Additional supporting information may be found online in the Supporting Information section at the end of the article.

Figure S1A. Representative microphotographs of interstitial fibrosis in the cancer therapy-related cardiac dysfunction (CTRCD) patients. Interstitial fibrosis was graded as follows: 0, absent; 1, <5%; 2, 5%–10%; 3, 10%–20%; and 4, >20% of the myocardium. Fibrosis comprised mainly of collagen component and stained as a blue area with Masson's trichrome stain. All microphotographs, original magnification ×400, Masson's trichrome stain.

Figure S1B. Representative microphotographs of replacement fibrosis in the cancer therapy-related cardiac dysfunction (CTRCD) patients. Replacement fibrosis was graded as follows: 0, absent; 1, <5%; 2, 5%–10%; 3, 10%–20%; and 4, >20% of the myocardium. Fibrosis is stained as blue area with Masson's trichrome stain. All microphotographs, original magnification ×100, Masson's trichrome stain.

Figure S1C. Representative microphotographs of nuclear atypia in the cancer therapy-related cardiac dysfunction (CTRCD) patients. Changes in cardiomyocytes under light microscopy were graded as follows: 0, absent; 1, mild; 2, moderate; 3, severe; and 4, extremely severe. In the CTRCD group, nuclear atypia showed grade 1–3. Grade 4 changes in cardiomyocytes were not observed among CTRCD patients. Grade 0 was found only in the control group. All microphotographs, original magnification ×400.

Figure S1D. Representative microphotographs of disarrangement of cardiomyocytes in the cancer therapy-related cardiac dysfunction (CTRCD) patients. Changes in cardiomyocytes under light microscopy were graded as follows: 0, absent; 1, mild; 2, moderate; 3, severe; and 4, extremely severe. Disarrangement of cardiomyocyte in CTRCD patients showed grade 1-4. Grade 0 of disarrangement was found only in the control group. All microphotographs, original magnification ×400.

Figure S1E. Representative microphotographs of sarcoplasmic rarefaction in cardiomyocytes in the cancer therapy-related cardiac dysfunction (CTRCD) patients. Changes in cardiomyocytes under light microscopy were graded as follows: 0, absent; 1, mild; 2, moderate; 3, severe; and 4, extremely severe. All microphotographs, original magnification ×400.

Figure S1F. Representative microphotographs of cardiomyocyte tapering of cardiomyocytes in the cancer therapy-related cardiac dysfunction (CTRCD) patients. Changes in cardiomyocytes under light microscopy were graded as follows: 0, absent; 1, mild; 2, moderate; 3, severe; and 4, extremely severe. In the CTRCD group, cardiomyocyte tapering showed grade 1-3. Grade 4 cardiomyocyte tapering was not observed in CTRCD patients. Grade 0 was found only in the control group.

Figure S1G. Representative microphotographs of cytoplasmic vacuolation of cardiomyocytes in the cancer therapy-related cardiac dysfunction (CTRCD) patients. Changes in cardiomyocytes under light microscopy were graded as follows: 0, absent; 1, mild; 2, moderate; 3, severe; and 4, extremely severe. In the CTRCD group, cytoplasmic vacuolation showed grade 1-3. Grade 4 cardiomyocyte tapering was not observed in CTRCD patients.

Figure S2. Evaluation of histological grading scores for fibrosis and changes in cardiomyocytes in autopsy cases including controls and those with oesophageal cancer, leukaemia, and lymphoma. Scoring ranged between 0 and 4 points, and higher scores indicated more severe changes. Autopsy cases exhibited significant histopathological changes including fibrosis (A, B) and changes in cardiomyocytes (C–G) in patients with cancer compared with the controls, similar to those observed in biopsy cases. *$p < 0.05$, **$p < 0.01$, ***$p < 0.001$ vs control.

Figure S3. Immunohistochemical evaluation of p53 and H3K27ac. Panels A and B show representative microphotographs of p53 and H3K27ac immunohistochemistry, respectively. Panels C and D show representative microphotographs of the scoring system used to determine the immunohisto-

chemical staining intensities of p53 and H3K27ac, respectively. **All microphotographs, original magnification ×400.**

Figure S4. The total score of cardiotoxicity risk score (CRS), histopathological features and histological scores (H-scores) for p53 and H3K27ac according to time from drug administration to CTRCD onset (short term, <4.2 years and long-term, >4.2 years). (A-C) The total score of CRS, medication score and the patient-related risk factor score did not differ between the two groups. Student's t test, *$p < 0.05$. (D, E) The total scores of fibrosis (interstitial and replacement) and the total scores of cardiomyocyte changes (nuclear atypia, disarrangement, rarefaction, tapering, and vacuolation) did not differ between the two groups. Student's t test, *$p < 0.05$. (F, G) The short-term group had a significantly higher H-score for H3K27ac than the long-term group, although no difference in H-score for p53 was observed. CTRCD, cancer therapy-related cardiac dysfunction

Figure S5. Comparison of cardiotoxicity risk score (CRS), histopathological features and histological scores (H-scores) for p53 and H3K27ac and left ventricular ejection fraction (LVEF) recovery between type 1 and type 2 CTRCD. (A) No difference in the total score of CRS was observed between the two groups. (B, C) The total fibrosis score (interstitial and replacement) and the total score of cardiomyocyte changes (nuclear atypia, disarrangement, rarefaction, tapering, and vacuolation) did not differ between the two groups. (D, E) H-score for p53 and H3K27ac did not differ between the two groups. (F) A comparison of LVEF at the time of biopsy and 1 year later between the short-term and long-term groups showed recovery of the LVEF even in those with type 2 CTRCD. CTRCD, cancer therapy-related cardiac dysfunction, LVEF, left ventricular ejection fraction.

Figure S6. Comparison of the changes in LVEF at the time of biopsy and 1 year after biopsy by dividing the CTRCD group into two groups based on the mean values of cardiotoxicity risk score (CRS), p53 H-score, total score of fibrosis (interstitial and replacement), and total score of cardiomyocyte changes (nuclear atypia, disarrangement, rarefaction, tapering, and vacuolation) at the time of biopsy. The group with values higher and lower than mean value was determined as the high- and low-group, respectively. There was no clear difference in LVEF between the two groups. CTRCD, cancer therapy-related cardiac dysfunction; LVEF, left ventricular ejection fraction.

Figure S7. Immunohistochemical evaluation of HAT1, p300 and MEF2A. Panels A to C show representative microphotographs of HAT1, p300 and MEF2A immunohistochemistry, respectively. Panels D to F show representative microphotographs of the scoring system used to determine the immunohistochemical staining intensities of HAT1, p300 and MEF2A, respectively. All microphotographs, original magnification ×400.

Figure S8. The histological score (H-score) of HAT1 and correlation with H3K27ac and p53 in autopsy samples from patients undergoing cancer treatment (divided into groups based on cancer type) and controls. (A) HAT1 H-scores were significantly higher in cases who died after treatment for various tumours than in the controls. Student's t test; *$p < 0.05$, **$p < 0.01$, ***$p < 0.001$ vs. control. (B, C) HAT1 was positively correlated with H3K27ac and p53; Spearman correlation performed.

Figure S9. The histological score (H-score) of p300 and correlation with H3K27ac and p53 in autopsy samples from patients undergoing cancer treatment (divided into groups based on cancer type) and controls. (A) There was no significant difference in p300 H-scores from controls in patients who died after treatment of various tumours. (B, C) There was no correlation between p300 and H3K27ac and p53 expression.

Figure S10. The histological score (H-score) of MEF2A and correlation with H3K27ac and p53 in autopsy samples from patients undergoing cancer treatment (divided into groups based on cancer type) and controls. (A) MEF2A H-score was significantly higher in leukaemia and lymphoma cases than in controls. Student's t test; *$p < 0.05$, **$p < 0.01$ vs. control. (B, C) There was no correlation between MEF2A and H3K27ac and p53 expression.

Figure S11. Comparison of time from death to autopsy and its association with immunohistological results. (A) No difference in time from death to autopsy was observed among autopsy cases. (B, C) No correlation was noted between time from death to autopsy and immunohistological results, such as p53 and H3K27ac.

Table S1. Detailed clinical background of patients with chemotherapy-related cardiac dysfunction (CTRCD) (endomyocardial biopsy cases).

Table S2. Detailed clinical background characteristics of control patients who underwent endomyocardial biopsy.

Table S3. Comparison of clinical background between patients with chemotherapy-related cardiac dysfunction (CTRCD) and controls (endomyocardial biopsy cases).

Table 4. Comparison of patient background between patients with early-onset (short-term) or late-onset (long-term) cancer therapy-related cardiac dysfunction (CTRCD).

Table S5. Detailed clinical background of cases autopsied after cancer treatment.

References

1. World Health Organization. Global health estimates 2015: deaths by cause, age, sex, by country and by region; 2016. p. 2000-2015.
2. Hahn VS, Lenihan DJ, Ky B. Cancer therapy-induced cardiotoxicity: basic mechanisms and potential cardioprotective therapies. *J Am Heart Assoc*. 2014; **3**: e000665.
3. Ewer MS, Ewer SM. Cardiotoxicity of anticancer treatments. *Nat Rev Cardiol*. 2015; **12**: 547–558.
4. Lipshultz SE, Franco VI, Miller TL, et al. Cardiovascular disease in adult survivors of childhood cancer. *Annu Rev Med*. 2015; **66**: 161–176.
5. Perez IE, Alam ST, Hernandez GA, et al. Cancer therapy-related cardiac dysfunction: an overview for the clinician. *Clin Med Insights Cardiol*. 2019; **13**: 1–11.
6. Lyon AR, Yousaf N, Battisti NML, et al. Immune checkpoint inhibitors and cardiovascular toxicity. *Lancet Oncol*. 2018; **19**: e447–e458.
7. Habibian M, Lyon AR. Monitoring the heart during cancer therapy. *Eur Heart J Suppl*. 2019; **21**: M44–M49.
8. Petek BJ, Greenman C, Herrmann J, et al. Cardio-oncology: an ongoing evolution. *Future Oncol*. 2015; **11**: 2059–2066.
9. Chatterjee K, Zhang J, Honbo N, Karliner JS. Doxorubicin cardiomyopathy. *Cardiology*. 2010; **115**: 155–162.
10. Ma W, Liu M, Liang F, et al. Cardiotoxicity of sorafenib is mediated through elevation of ROS level and CaMKII activity and dysregulation of calcium homeostasis. *Basic Clin Pharmacol Toxicol*. 2020; **126**: 166–180.
11. Gilsbach R, Schwaderer M, Preissl S, et al. Distinct epigenetic programs regulate cardiac myocyte development and disease in the human heart in vivo. *Nat Commun*. 2018; **9**: 391.
12. Pfeffer TJ, Pietzsch S, Hilfiker-Kleiner D. Common genetic predisposition for heart failure and cancer. *Herz*. 2020; **45**: 632–636.
13. Herrmann J, Lerman A, Sandhu NP, et al. Evaluation and management of patients with heart disease and cancer: cardio-oncology. *Mayo Clin Proc*. 2014; **89**: 1287–1306.
14. Lubieniecka JM, Graham J, Heffner D, et al. A discovery study of daunorubicin induced cardiotoxicity in a sample of acute myeloid leukaemia patients prioritizes P450 oxidoreductase polymorphisms as a potential risk factor. *Front Genet*. 2013; **4**: 231.
15. Choueiri TK, Mayer EL, Je Y, et al. Congestive heart failure risk in patients with breast cancer treated with bevacizumab. *J Clin Oncol*. 2011; **29**: 632–638.
16. Zamorano JL, Lancellotti P, Rodriguez Muñoz D, et al. ESC Position Paper on cancer treatments and cardiovascular toxicity developed under the auspices of the ESC Committee for Practice Guidelines: the task force for cancer treatments and cardiovascular toxicity of the European Society of Cardiology (ESC). *Eur Heart J*. 2016; **37**: 2768–2801.
17. Varnava AM, Elliott PM, Sharma S, et al. Hypertrophic cardiomyopathy: the interrelation of disarray, fibrosis, and small vessel disease. *Heart*. 2000; **84**: 476–482.
18. World Medical Association Declaration of Helsinki. Recommendations guiding physicians in biomedical research involving human subjects. *Cardiovasc Res*. 1997; **35**: 2–3.
19. Cardinale D, Colombo A, Bacchiani G, et al. Early detection of anthracycline cardiotoxicity and improvement with heart failure therapy. *Circulation*. 2015; **131**: 1981–1988.
20. Van Den Broeck A, Brambilla E, Moro-Sibilot D, et al. Loss of histone H4K20 trimethylation occurs in preneoplasia and influences prognosis of non-small cell lung cancer. *Clin Cancer Res*. 2008; **14**: 7237–7245.
21. Mohan N, Jiang J, Dokmanovic M, Wu WJ. Trastuzumab-mediated cardiotoxicity: current understanding, challenges, and frontiers. *Antib Ther*. 2018; **1**: 13–17.
22. Thavendiranathan P, Negishi T, Somerset E, et al. Strain-guided management of potentially cardiotoxic cancer therapy. *J Am Coll Cardiol*. 2021; **77**: 392–401.
23. Santoro C, Esposito R, Lembo M, et al. Strain-oriented strategy for guiding cardioprotection initiation of breast cancer patients experiencing cardiac dysfunction. *Eur Heart J Cardiovasc Imaging*. 2019; **20**: 1345–1352.
24. Demissei BG, Adusumalli S, Hubbard RA, et al. Cardiology involvement in patients with breast cancer treated with trastuzumab. *JACC CardioOncol*. 2020; **2**: 179–189.
25. Ryberg M, Nielsen D, Skovsgaard T, et al. Epirubicin cardiotoxicity: an analysis of 469 patients with metastatic breast cancer. *J Clin Oncol*. 1998; **16**: 3502–3508.
26. Meijers WC, de Boer RA. Common risk factors for heart failure and cancer. *Cardiovasc Res*. 2019; **115**: 844–853.
27. Lawson CA, Zaccardi F, Squire I, et al. Risk factors for heart failure 20-year population-based trends by sex, socioeconomic status, and ethnicity. *Circ Heart Fail*. 2020; **13**: e006472.
28. Morita H, Komuro I. Heart failure as an aging-related phenotype. *Int Heart J*. 2018; **59**: 6–13.
29. Tamagawa H, Oshima T, Numata M, et al. Global histone modification of H3K27 correlates with the outcomes in patients with metachronous liver metastasis of colorectal cancer. *Eur J Surg Oncol*. 2013; **39**: 655–661.
30. Melo CA, Drost J, Wijchers PJ, et al. eRNAs are required for p53-dependent enhancer activity and gene transcription. *Mol Cell*. 2013; **49**: 524–535.
31. Zhang Y, Qian M, Tang F, et al. Identification and analysis of p53-regulated enhancers in hepatic carcinoma. *Front Bioeng Biotechnol*. 2020; **8**: 668.
32. Sammons MA, Zhu J, Drake AM, Berger SL. TP53 engagement with the genome occurs in distinct local chromatin environments via pioneer factor activity. *Genome Res*. 2015; **25**: 179–188.
33. Haggerty CM, Damrauer SM, Levin MG, et al. Genomics-first evaluation of heart disease associated with titin-truncating variants. *Circulation*. 2019; **140**: 42–54.
34. Li S, Zhang C, Liu N, et al. Titin-truncating variants are associated with heart failure events in patients with left ventricular non-compaction cardiomyopathy. *Clin Cardiol*. 2019; **42**: 530–535.
35. Tayal U, Prasad S, Cook SA. Genetics and genomics of dilated cardiomyopathy and systolic heart failure. *Genome Med*. 2017; **9**: 20.
36. Tobita T, Nomura S, Fujita T, et al. Genetic basis of cardiomyopathy and the genotypes involved in prognosis and left ventricular reverse remodeling. *Sci Rep*. 2018; **8**: 1.